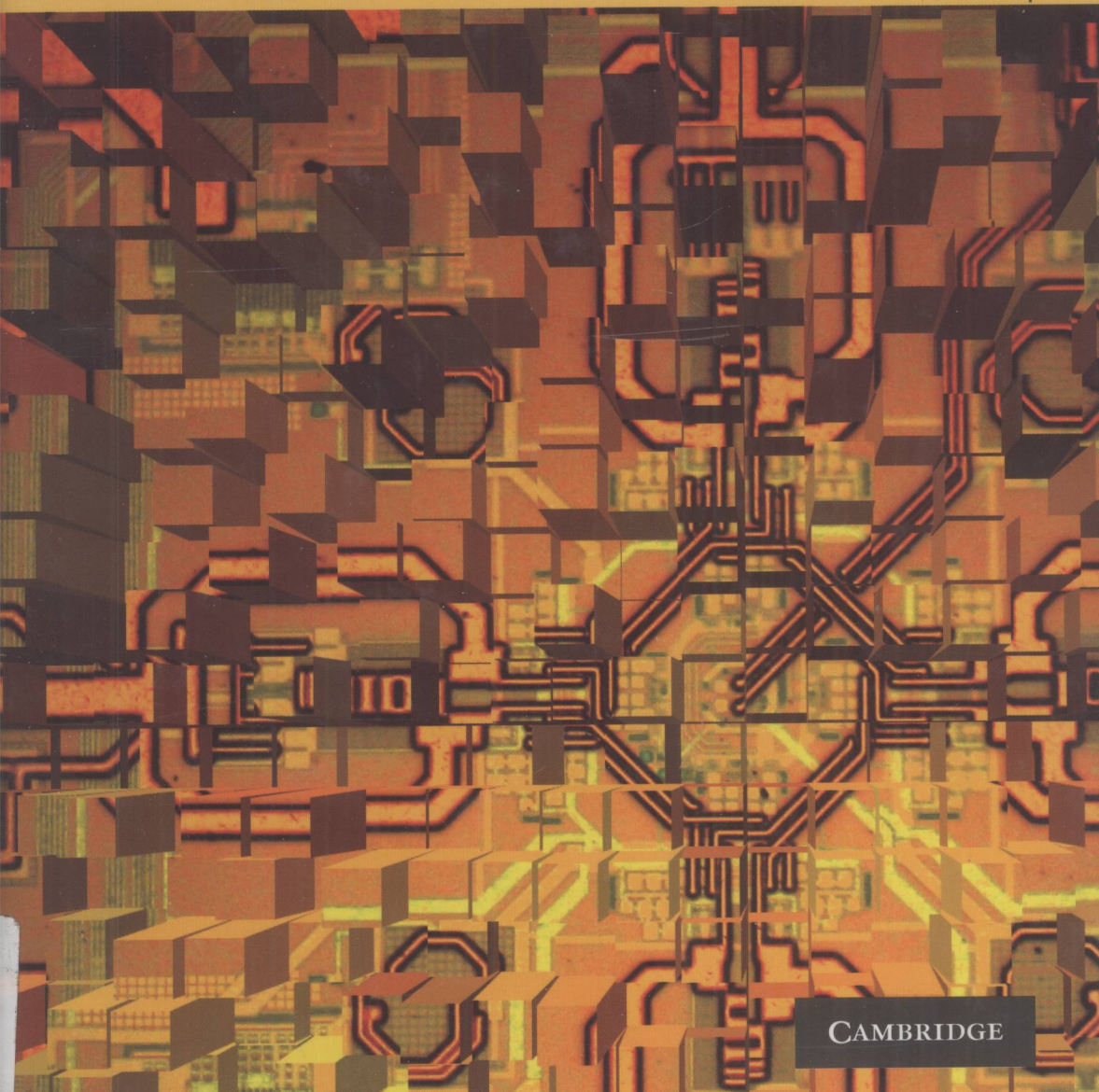


Integrated Frequency Synthesizers for Wireless Systems

Andrea Lacaita, Salvatore Levantino,
and Carlo Samori



CAMBRIDGE

TN74
L128

Integrated Frequency Synthesizers for Wireless Systems

Andrea Lacaita, Salvatore Levantino, and
Carlo Samori

Politecnico di Milano, Italy



CAMBRIDGE
UNIVERSITY PRESS



E2008000282

CAMBRIDGE UNIVERSITY PRESS

Cambridge, New York, Melbourne, Madrid, Cape Town, Singapore, São Paulo

Cambridge University Press

The Edinburgh Building, Cambridge CB2 8RU, UK

Published in the United States of America by Cambridge University Press, New York

www.cambridge.org

Information on this title: www.cambridge.org/9780521863155

© Cambridge University Press 2007

This publication is in copyright. Subject to statutory exception and to the provisions of relevant collective licensing agreements, no reproduction of any part may take place without the written permission of Cambridge University Press.

First published 2007

Printed in the United Kingdom at the University Press, Cambridge

A catalogue record for this publication is available from the British Library

ISBN 978-0-521-86315-5 hardback

Integrated Frequency Synthesizers for Wireless Systems

The increasingly demanding performance requirements of communications systems, as well as problems posed by the continued scaling of silicon technology, present numerous challenges for the design of frequency synthesizers in modern transceivers.

This book contains everything you need to know for the efficient design of frequency synthesizers for today's communications applications. If you need to optimize performance and minimize design time, you will find this book invaluable.

Using an intuitive yet rigorous approach, the authors describe simple analytical methods for the design of phase-locked loop (PLL) frequency synthesizers using scaled silicon CMOS and bipolar technologies. The entire design process, from system-level specification to layout, is covered comprehensively. Practical design examples are included, and implementation issues are addressed.

A key problem-solving resource for practitioners in integrated-circuit design, the book will also be of interest to researchers and graduate students in electrical engineering.

Andrea Lacaita is Full Professor of Electrical Engineering at the Politecnico di Milano, Italy.

Salvatore Levantino is Assistant Professor of Electrical Engineering at the Politecnico di Milano.

Carlo Samori is Associate Professor of Electrical Engineering at the Politecnico di Milano.

Preface

The phase-locked loop (PLL) concept is about 70 years old and a wealth of literature is already available on the subject. Someone may therefore ask why another book about PLLs.

The first reason is related to the specific application considered here, namely the silicon integration of frequency synthesizers. Classical texts do not deal in depth with issues related to the design of frequency synthesizers in modern transceivers. In particular, the design guidelines and the performance of some important building blocks and their impact on the whole system are sometimes barely mentioned. The attempt, here, has been instead to provide a broad description of the most typical circuit topologies of voltage-controlled oscillators, frequency dividers and phase and frequency detectors, and to discuss their performance in terms of power consumption, phase noise, spurs, and so forth. A chapter is also devoted to integrated passive components, such as varactors and inductors, since the ability to optimize their performance judiciously is becoming a key skill required of the RF designer.

The second reason is that the book attempts to provide an alternative approach to PLL theory and design. After years of research and study on the subject, the authors propose an analysis methodology that is both rigorous and intuitive. The ability to simplify the picture and to address schematically the impact of complex, often non-linear, effects is a fundamental skill of any good engineer. The PLL is a good training example for the designer. In this respect, the book provides many examples of models, starting from a schematic and simplified description of the circuit operation and then leading to estimates, which are compared with simulation results. These examples are intended not only to provide a deeper insight into complex and intriguing effects, but also to encourage students and young analogue designers to keep exercising the ability to figure out the consequences of technical choices before performing circuit simulations.

The book starts with three chapters addressing the PLL as a system. Chapter 1 points out the typical requirements of the frequency synthesizer in RF systems. Chapter 2 covers some PLL basics. It does not deal with the whole PLL theory, which is analyzed in depth in many classical books. The chapter highlights only the concepts needed for understanding the subsequent topics. Chapter 3 finally analyzes fractional-division PLLs, which are seldom discussed in other texts.

Chapters 4 to 9 are then devoted to discussing in detail the design issues related to the PLL building blocks. Chapters 4 to 7 deal with voltage-controlled oscillators and their practical implementations in bipolar and CMOS technologies, including resonator design and layout. Chapters 8 and 9 are focused on the design of programmable dividers and phase-comparison circuits, including issues related to non-linearities.

Acknowledgments

The research activity behind this book has been in progress for more than ten years. It was made possible thanks to the financial support provided by the Italian Ministry of Universities and Research and by industry. In this respect, many thanks go to Mario Paparo of STMicroelectronics (Catania, Italy), Maurizio Pagani of Ericsson Lab (Vimodrone, Italy), and to Mihai Banu of the (formerly) Silicon Circuit Research Department of Bell Laboratories (Murray Hill, NJ), for their strong support.

The authors are indebted to all their past graduate students, Mr Francesco Villa, Dr Alfio Zanchi, Dr Andrea Bonfanti, Dr Luca Romanò, Dr Stefano Pellerano, Dr Marco Milani and Dr Luigi Panseri, who shared the excitements of this research and contributed to most of the understanding reported in the following pages. The authors are also extremely grateful to their current Ph.D. students, Paolo Madoglio and Marco Zanuso, who worked out the examples and the simulations, providing critical revisions of the text. Clearly, only the authors are responsible for any errors that may still be present.

Contents

	<i>Preface</i>	page vii
	<i>Acknowledgments</i>	viii
1	Local oscillator requirements	1
	1.1 AM and PM signals	2
	1.2 Effect of phase noise and spurs	6
	1.3 Frequency accuracy	9
	1.4 Switching speed	12
	1.5 References	12
2	Phase-locked loops	14
	2.1 Basics	14
	2.2 PLL for frequency synthesis	23
	2.3 Discrete-time and non-linearity effects	32
	2.4 Spectral purity: spurs and phase noise	38
	2.5 References	47
3	Fractional-N PLLs	49
	3.1 Beyond the integer- N approach	49
	3.2 Fractional- N division	50
	3.3 $\Delta\Sigma$ control of division factor	58
	3.4 $\Delta\Sigma$ fractional- N PLL	65
	3.5 References	72
4	Electronic oscillators	74
	4.1 Introduction	74
	4.2 Principles of LC oscillators	74
	4.3 Single-transistor oscillators	82
	4.4 Differential oscillators	91
	4.5 References	101
5	Noise in oscillators	103
	5.1 Introduction	103
	5.2 Linear and time-invariant model	103
	5.3 Noise–power trade-off and scaling issues	105

	5.4 Time-variant models	108
	5.5 Application to some practical cases	116
	5.6 Additional issues in low-phase-noise design	131
	5.7 References	131
6	Reactive components in oscillators	133
	6.1 Introduction	133
	6.2 Integrated inductors	133
	6.3 Inductor topologies	141
	6.4 Integrated varactors	146
	6.5 Switched tuning	153
	6.6 References	155
7	Noise up-conversion in VCOs	157
	7.1 Introduction	157
	7.2 Tuning curve and sensitivity coefficients	157
	7.3 Noise up-conversion from varactors	161
	7.4 Topologies and methods to minimize for up-conversion	166
	7.5 Other mechanisms of noise up-conversion	175
	7.6 References	180
8	Frequency division	182
	8.1 Introduction	182
	8.2 Digital frequency dividers	182
	8.3 Programmable dividers	188
	8.4 Dual-modulus prescalers	193
	8.5 Circuit implementation	198
	8.6 Noise in digital dividers	204
	8.7 References	209
9	Phase comparison	211
	9.1 Introduction	211
	9.2 Phase comparison path	211
	9.3 Phase/frequency detectors	214
	9.4 Charge pump	224
	9.5 Phase-detection noise	229
	9.6 References	234
	<i>Index</i>	236

1 Local oscillator requirements

Personal wireless communications have represented, for the microelectronic industry, the market with the largest growth rate in the last ten years. The key for such a boom has been the standardization effort made by several organizations and the replacement of compound semiconductors with silicon technology in building radio front ends. This advancement was made possible by joint progress in communication theory, devices technology and system and circuit design. Silicon technology made it possible to attain lower fabrication costs, owing to the large production volumes and to the possibility of implementing complex digital functions together with radio-frequency (RF) signal manipulations, lowering the number of off-chip components.

Initially in the 1990s, cellular systems have been the driving application for this technology evolution. Further generations of cellular telephones have introduced the possibility of communicating not only by voice but also with text messages, images and videos. Later, a number of wireless technologies have emerged, not strictly belonging to the class of communication systems. Some examples are wireless local-area networks (WLAN), sensor networks, wireless USB applications and automotive radar.

Table 1.1 summarizes various high-level characteristics of the most common communication standards. Despite the variety of modulation formats and access methods, the basic structure of a typical transceiver has remained as shown in Figure 1.1. In both the receiving and the transmitting branch, frequency conversions are performed to move the signal from the RF band to the base band and vice versa. Up-conversions and down-conversions can be performed in one or more steps, and amplification and filtering can be distributed differently along the chains. Whatever architecture is adopted, the core of these operations is always the multiplication of the signal by sinusoids provided by the local oscillator (LO). This stage is therefore a key element of the overall transceiver.

What Table 1.1 does not point out is that the information is travelling in a ‘hostile’ time-varying channel, affected by noise and strong interferences, Doppler effects and multi-path fading. These effects impose severe requirements on the receiver and transmitter performance. Just to mention a popular example, the sensitivity (i.e., the minimum signal power to be detected at the antenna) in a GSM receiver is about -102 dBm. On the other hand, the largest blocker or interferer that the system must tolerate is 0 dBm. It follows that the GSM receiver has to be able to detect a weak signal even in the presence of an interferer with a power of about 10 orders of magnitude larger. Such a stringent requirement is quite uncommon in other fields of electrical engineering.

Table 1.1 *Characteristics of some communication standards*

Standard	RX band (MHz)	TX band (MHz)	Channel spacing (kHz)	Multiple access	Modulation
GSM	925–960	880–915	200	TDMA/FDMA	GMSK
DCS	1805–1880	1710–1785	200	TDMA/FDMA	GMSK
IS-95	869–894	824–849	1 250	CDMA/FDMA	QPSK/OQPSK
IS-54	869–894	824–849	30	TDMA/FDMA	$\pi/4$ -DQPSK
IS-136	1930–1990	1850–1910	30	TDMA/FDMA	$\pi/4$ -DQPSK
UMTS	2110–2170	1920–1980	5 000	W-CDMA	QPSK
Bluetooth	2400–2483.5		1 000	TDMA/FDMA	GFSK
802.11a	5180–5320, 5745–5805		20 000	TDMA/FDMA	OFDM
802.11b	2400–2483.5		20 000	CSMA	DSSS-CCK

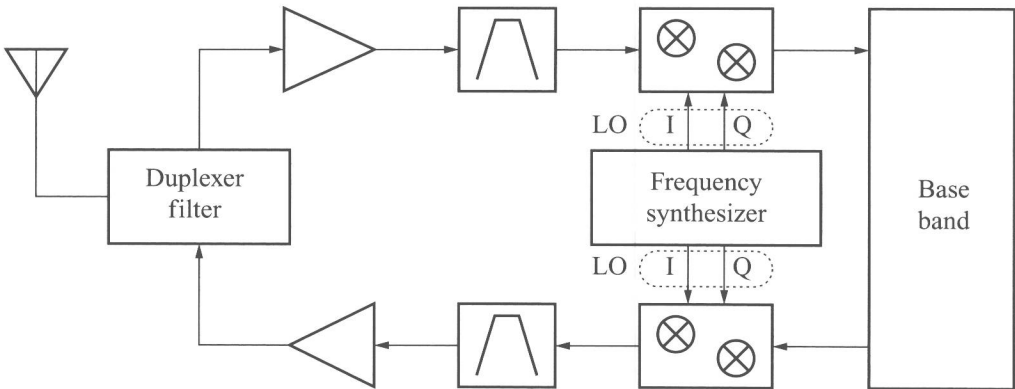


Figure 1.1 Generic structure of a transceiver

To achieve such extreme performance, the architecture of the transceiver has to be carefully selected, depending on the communication standard specifications, [1–3] and the design of its building blocks has to be carefully pursued. The local oscillator has to match tight levels of spectral purity so that the quality of the received signal is preserved, and it must be able to change its frequency so that various channels of the receiver band can be converted to the same frequency. For this reason, the local oscillator is, in practice, a frequency synthesizer, or a circuit that is able to synthesize harmonic reference waveforms in a certain frequency range. Several implementations of this stage exist; however, the phase-locked loop (PLL) is the most common.

1.1 AM and PM signals

The signals generated by the local oscillator are ideally sinusoidal or harmonic:

$$V_0(t) = A_0 \cdot \cos(\omega_0 t + \phi_0),$$

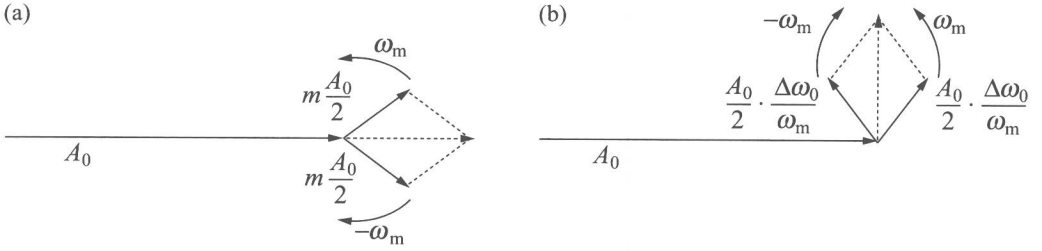


Figure 1.2 (a) Amplitude-modulated carrier and (b) phase-modulated carrier

where the amplitude A_0 , the frequency ω_0 and the phase ϕ_0 are constant. The ‘angular frequency’ ω (measured in rad/s) will be referred to simply as ‘frequency’. It will be clear from the symbol (either ω or f), and from the context, whether the term frequency refers to the angular frequency or to the actual frequency $\omega/2\pi$ (measured in Hz).

In a real synthesizer, the signal amplitude and frequency can suffer from modulation, owing to the presence of noise or disturbances. An amplitude-modulated (AM) signal may be written as:

$$V_0(t) = A_0 \cdot [1 + m \cdot \cos(\omega_m t)] \cdot \cos(\omega_0 t + \phi_0).$$

The spectral components of the AM signal are better identified, when the previous expression is written as:

$$V_0(t) = A_0 \cdot \cos(\omega_0 t + \phi_0) + \frac{mA_0}{2} \cdot \cos[(\omega_0 - \omega_m)t + \phi_0] + \frac{mA_0}{2} \cdot \cos[(\omega_0 + \omega_m)t + \phi_0].$$

The spectrum has two side tones at an offset $\pm \omega_m$ from the carrier at ω_0 . Owing to the amplitude variations, the AM signal has a power larger than the original unmodulated harmonic. Using phasor notation and taking the carrier as a reference, the two tones will appear as in Figure 1.2(a). In most typical cases, $m \ll 1$ and $\omega_m \ll \omega_0$.

On the other hand, a frequency-modulated (FM) signal may be denoted as $\omega(t) = \omega_0 + \Delta\omega_0 \cdot \cos(\omega_m t)$. Since the phase is the integral of the frequency, the signal is also modulated in phase (PM). It is:

$$V_0(t) = A_0 \cos \left[\omega_0 t + \phi_0 + \frac{\Delta\omega_0}{\omega_m} \sin(\omega_m t) \right].$$

Since the amplitude is constant, this time the modulated signal has the same power as the original, unmodulated harmonic. The modulated phase is $\phi(t) = (\Delta\omega_0/\omega_m) \cdot \sin(\omega_m t)$. Under the assumption of a small modulation index ($\Delta\omega_0/\omega_m \ll 1$ rad, it is $\cos[\phi(t)] \simeq 1$,

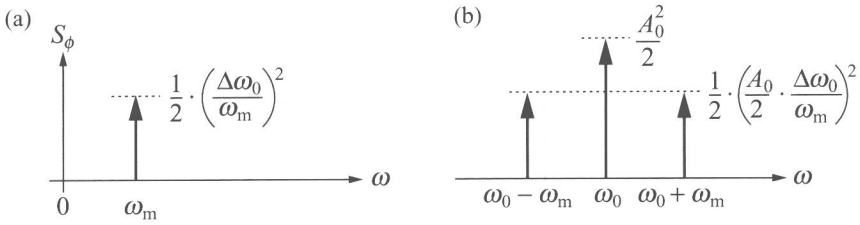


Figure 1.3 Power spectra (a) of the phase signal and (b) of the corresponding voltage signal

$\sin[\phi(t)] \simeq \phi(t)$, so the signal $V_0(t)$ can be approximated as:

$$\begin{aligned}
 V_0(t) &\cong A_0 \cos(\omega_0 t + \phi_0) - A_0 \sin(\omega_0 t + \phi_0) \cdot \frac{\Delta\omega_0}{\omega_m} \sin(\omega_m t) \\
 &= A_0 \cos(\omega_0 t + \phi_0) - \frac{A_0}{2} \cdot \frac{\Delta\omega_0}{\omega_m} \cos[(\omega_0 - \omega_m)t] \\
 &\quad + \frac{A_0}{2} \cdot \frac{\Delta\omega_0}{\omega_m} \cos[(\omega_0 + \omega_m)t].
 \end{aligned} \tag{1.1}$$

The approximation is usually referred to as narrow-band FM. Figure 1.2(b) shows the two side tones in the carrier frame. From the above assumptions, the carrier appears modulated not only in phase but also in amplitude. The resulting phasor has peak phase deviation equal to $\arctan(\Delta\omega_0/\omega_m)$ and peak amplitude equal to $A_0 \cdot \sqrt{1 + (\Delta\omega_0/\omega_m)^2}$, which approach $(\Delta\omega_0/\omega_m)$ and A_0 , respectively, under the narrow-band FM approximation.

It is interesting to compare the power spectrum¹ S_ϕ of the phase signal $\phi(t)$ and the spectrum of the voltage signal $V_0(t)$. Since the phase signal is harmonic, its power spectrum is a δ -like function at ω_m , with area equal to the mean square value of the phase signal $(1/2)(\Delta\omega_0/\omega_m)^2$. It is schematically represented in Figure 1.3(a). Figure 1.3(b) shows the power spectrum of V_0 as derived from (1.1). The ratio between the power of each side tone and the power of the carrier is given by:

$$\frac{\text{Power of the single tone}}{\text{Carrier power}} = \frac{\left(\frac{A_0}{2} \cdot \frac{\Delta\omega_0}{\omega_m}\right)^2 \cdot \frac{1}{2}}{\frac{A_0^2}{2}} = \frac{1}{4} \cdot \left(\frac{\Delta\omega_0}{\omega_m}\right)^2. \tag{1.2}$$

That is equal to half the power of S_ϕ . The tones due to a frequency modulation at ω_m are referred to as spurious tones or spurs. The above ratio is often called the spurious free dynamic range (SFDR). It is expressed in dB, and labelled as dBc, i.e., dB with respect to the carrier. For a given frequency deviation $\Delta\omega_0$, the S_ϕ amplitude is inversely proportional to the square of the offset ω_m . If the signal is both amplitude-modulated and frequency-modulated at ω_m , the voltage spectrum shows two side tones of different amplitudes.

The same arguments leading to (1.2) can be used to address the impact of every noise spectral component affecting the carrier frequency. The noise may be regarded as the superposition of tones $\Delta\omega_0 \cdot \cos(\omega_m t)$. If the frequency noise is white, the peak frequency

¹ Here and in the following the power spectra are intended to be unilateral: they are defined only for positive frequencies.

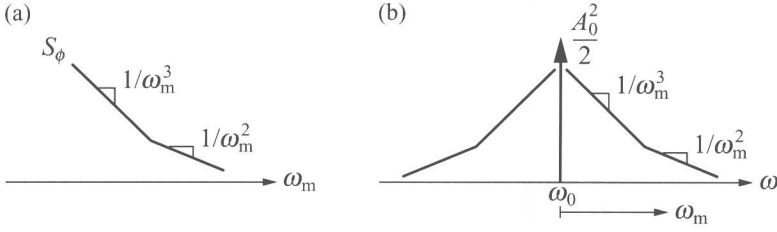


Figure 1.4 (a) Phase-noise spectrum and (b) corresponding voltage spectrum

deviation $\Delta\omega_0$ is constant. Since the phase is the integral of the frequency, the phase–power spectrum $S_\phi(\omega_m)$ shows a $1/\omega_m^2$ tail (-20 dB/decade slope in Figure 1.4(a)). If, instead, the frequency noise has a $1/f$ (flicker) component, the $\Delta\omega_0$ amplitude goes as $1/\omega_m$, and $S_\phi(\omega_m)$ shows a $1/\omega_m^3$ dependence (-30 dB/decade).

Under the small-angle approximation, the corresponding voltage signal features the same $S_\phi(\omega_m)$ shape (Figure 1.4(b)). The only difference is that it has two tails, for both positive and negative frequency offsets ω_m from the carrier. The voltage–power spectral density at $\omega_0 \pm \omega_m$ is $S_V(\omega_0 \pm \omega_m) \cong (S_\phi(\omega_m)/2) \cdot (A_0^2/2)$. Since the noise level of the sideband depends on the carrier power, the noise level is typically quantified as the noise power in a 1 Hz bandwidth at offset $+\omega_m$ or $-\omega_m$ from ω_0 divided by the carrier power. This figure is denoted as the single-sideband-to-carrier ratio (SSCR), or \mathcal{L} (L script):

$$\mathcal{L}(\omega_m) = \frac{\text{Power in 1 Hz bandwidth}}{\text{Carrier power}} = \frac{S_V(\omega_0 \pm \omega_m)}{A_0^2/2} \cong \frac{S_\phi(\omega_m)}{2} \text{ (dBc/Hz)}. \quad (1.3)$$

A factor of 1 Hz multiplies both S_V and S_ϕ and sets the correct physical dimensions. The term phase noise is often used indiscriminately for \mathcal{L} and for S_ϕ , even though the two quantities are different (clearly, S_ϕ is 3 dB larger than \mathcal{L}). The phase noise is the most important characteristic of an oscillator used for RF applications.

It may be noticed that the power of the oscillator output voltage, which is obtained as the integral of the power spectral density² S_V in Figure 1.4(b), is infinite. This unphysical result comes from the small-angle approximation $\phi(t) \ll 1$ rad, which has been used to derive (1.1). At small offsets ω_m , S_ϕ goes to infinity, $\phi(t)$ does not satisfy the inequality $\phi(t) \ll 1$ rad any more and the voltage spectrum differs from S_ϕ . If the frequency noise is white, it can be shown that the voltage spectrum has a Lorentzian shape and its integral is equal to the power of the ideal carrier. [4]

For the approximation $\mathcal{L}(\omega_m) \cong S_\phi(\omega_m)/2$ to hold down to a certain frequency f_1 it must be:

$$\int_{f_1}^{\infty} S_\phi(2\pi f_m) \cdot df_m \ll 1 \text{ (rad)}^2.$$

² Because the power spectral density of a signal is typically defined as the signal power in a 1 Hz bandwidth, the frequency f and not the angular frequency has to be used in the integration of the spectral density.

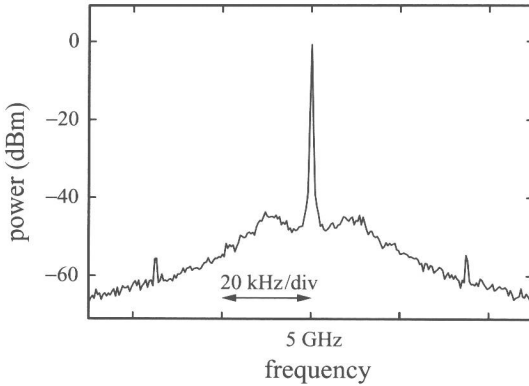


Figure 1.5 A typical PLL output spectrum

In RF oscillators for wireless systems, it is typically satisfied down to 100 Hz, which is a frequency limit low enough for most purposes. Equation (1.3) will therefore always be used in the following. Moreover, it should be taken into account that the oscillator is not a stand-alone circuit, but it is embedded in the PLL. In the next chapter, it will be shown that S_ϕ at the PLL output is high-pass filtered, for offsets smaller than the bandwidth of the PLL itself. The same holds for the S_V spectrum, thus removing the potential divergence close to the carrier. Figure 1.5 shows the typical S_V output spectrum of a PLL with a 10 kHz bandwidth. Note that the tails stop at about 10 kHz from the carrier and the spectrum does not show any divergence close to the carrier frequency. Two spurious tones at ± 35 kHz indicate a residual frequency (phase) modulation of the carrier.

1.2 Effect of phase noise and spurs

Both phase noise and spurs affect the spectral purity of the local oscillator. While the phase noise is characterized by a distributed spectrum, the spurs are instead well-defined undesired tones. Depending on the applications, care must be devoted to limit either the ‘spot’ value of the spectrum at a given frequency or the integral of the phase–power spectral density over a given spectral range.

Let us consider the simplified block diagram of a transceiver in Figure 1.1. In the receiving path, the signal at RF is down-converted to the base band or to an intermediate frequency (IF) by the mixer driven by the LO. Let us suppose that a strong interferer (blocker) at an offset ω_m is received together with the signal. This is a very realistic situation, taking place when the receiver also picks up the signal of a nearby transmitter. Assuming an ideal LO with a δ -like spectrum, the blocker will be down-converted at ω_m from the signal, and filtered out. When the LO phase noise is taken into account, the outcome changes drastically. The spectra of the two down-converted signals can overlap (Figure 1.6) and the desired signal can be corrupted by the tail of the interferer. This effect is called reciprocal mixing and degrades the signal-to-noise ratio (SNR). More quantitatively, the SNR may be

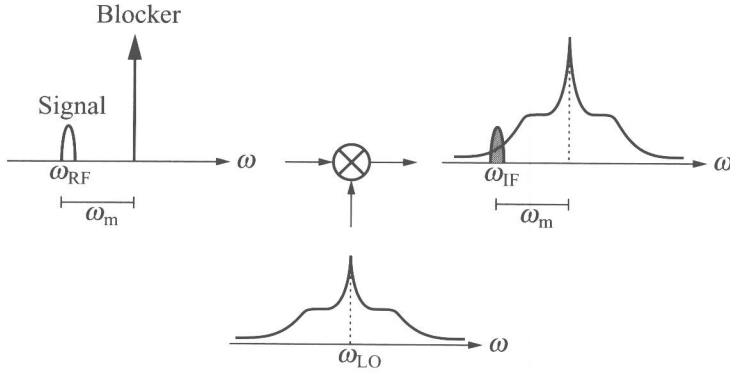


Figure 1.6 Reciprocal mixing

written as:

$$\text{SNR} = \frac{P_S}{\mathcal{L}(\omega_m) \cdot B \cdot P_B}$$

where P_S and P_B are the powers of the desired signal and the blocker, respectively, and B is the signal bandwidth. The expression may be converted into dB, leading to:

$$\text{SNR}_{\text{dB}} = (P_S|_{\text{dBm}} - P_B|_{\text{dBm}}) - \mathcal{L}(\omega_m)|_{\text{dBc}} - 10 \cdot \log_{10} B. \quad (1.4)$$

Typically, a minimum value of SNR is required. If the ratio between the maximum blocker and the minimum signal power is large, the phase noise specification, \mathcal{L} , can be severe. That is the case of GSM, which is discussed in Example 1.1.

If an LO spur occurs at the same frequency offset between the signal and the blocker, the reciprocal mixing can be even more problematic. The blocker would be down-converted by the spur to the same IF of the signal. The signal-to-interference ratio can now be written by using the SFDR defined in (1.2):

$$\text{SNR}_{\text{dB}} = (P_S|_{\text{dBm}} - P_B|_{\text{dBm}}) - \text{SFDR}_{\text{dB}}.$$

Therefore, the occurrence of blockers defines the maximum level of the spot values of the LO phase noise spectrum at some well-defined frequencies.

Of course, even if blockers are not present, the LO phase noise corrupts the signal anyhow and leads to SNR degradation or detection loss. In this case, the SNR will be a function of the phase noise power, that is the integral of the LO spectrum. Let us consider, as an example, a generic M-QAM modulated carrier. It can be written as:

$$s(t) = \sum_k a_k \cdot p(t - kT) \cdot \cos(\omega_0 t) - \sum_k b_k \cdot p(t - kT) \cdot \sin(\omega_0 t),$$

where (a_k, b_k) are the symbols transmitted in the I/Q paths and $p(t)$ is the normalized Nyquist pulse. The signal $s(t)$ can be regarded as an amplitude-modulated and phase-modulated carrier at ω_0 and complex envelope $(a_k + jb_k) \cdot p(t - kT)$. It is:

$$s(t) = \text{Re} \left[\sum_k (a_k + jb_k) \cdot p(t - kT) \cdot e^{j\omega_0 t} \right].$$

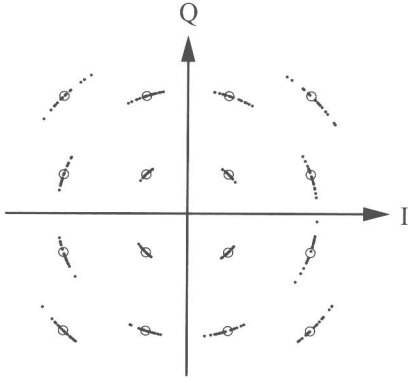


Figure 1.7 A 16-QAM constellation affected by phase noise

After down-conversion, coherent demodulation and sampling, the transmitted symbols (a_k, b_k) , or constellation, are identified. Let us suppose that the LO in the transmitter is affected by phase noise $\phi_n(t)$. The transmitted signal $s(t)$ thus becomes:

$$s(t) = \sum_k a_k \cdot p(t - kT) \cdot \cos(\omega_0 t + \phi_n(t)) - \sum_k b_k \cdot p(t - kT) \cdot \sin(\omega_0 t + \phi_n(t)),$$

or, equivalently:

$$s(t) = \text{Re} \left[\sum_k (a_k + jb_k) \cdot e^{j\phi_n(t)} \cdot p(t - kT) \cdot e^{j\omega_0 t} \right].$$

Therefore, the demodulated signal will be $(a_k + jb_k) \cdot \exp[j\phi_n(t)]$, i.e., the received constellation is rotated by $\phi_n(t)$. Of course, this discussion holds even if the LO of the receiver is affected by phase noise. The phase-noise contributions of the receiver and the transmitter are added in power to get the overall phase noise. Figure 1.7 depicts, qualitatively, the effect of phase noise on a 16-QAM constellation. The detection loss is related to the r.m.s. value of $\phi_n(t)$. It is denoted as σ_ϕ and is given by:

$$\sigma_\phi = \sqrt{\int_{f_1}^{f_2} S_\phi(2\pi f_m) \cdot df_m}.$$

The phase-noise power spectral density is typically integrated between frequencies f_1 and f_2 . The first lower limit is set by the bandwidth of a frequency-error correction algorithm, which is typically adopted in the digital base-band subsystem. The upper frequency f_2 is set approximately by the signal bandwidth. In practice, a phase noise at frequency offsets larger than the channel bandwidth has a negligible impact on detection loss. Even the spurious tones present in the phase spectrum contribute to the r.m.s. phase deviation σ_ϕ and should be accounted for in the design.

1.3 Frequency accuracy

The frequency generated by a synthesizer has to be extremely accurate. For instance, the mobile terminal in the GSM standard must transmit signals with frequency accuracy better than 0.1 parts per million (p.p.m.), which means an error of 100 Hz for a 1 GHz carrier frequency. This value is far beyond the performance of commercially available components. If the LO signal is locked to an off-chip temperature-controlled crystal oscillator (TCXO), the achievable frequency accuracy cannot be better than 20 ppm.

To reach the target performance, the base station broadcasts a tone for a short time (frequency control burst), which is derived from a more accurate frequency reference. The frequency error between the received tone and the mobile terminal LO is detected at the base band by a maximum-likelihood estimation algorithm. Frequency correction is then performed either by acting on the crystal oscillator, or by rotating the received constellation (that is by multiplying the base-band complex signal by $\exp[j\Delta\omega \cdot t]$, $\Delta\omega$ being the frequency error). The former approach is adopted in GSM terminals, [5] while the latter can be found in some examples of WLAN clients.

A third option is to act on the input control of the frequency synthesizer, which generates the mobile terminal LO. This method requires a very-fine-tuning synthesizer, which can be achieved by the fractional- N PLL discussed in Chapter 3.

Example 1.1 Phase noise in GSM terminals

The GSM standard is the popular standard for cellular systems, which operates in the 900 MHz and 1800 MHz RF bands. The main characteristic of the GSM standard is its very tight blocking specification. The transceiver has to operate with blockers, which can be 76 dB more intense than the desired signal. Figure 1.8 shows the blocking signal level.

The GSM reference sensitivity has to be -102 dBm, but the receiver must meet the bit error rate (BER) for a useful signal 3 dB above the reference sensitivity in the presence of blockers, that is at -99 dBm. [6] Therefore, the LO phase noise specifications are set by the reciprocal mixing and not by the integral noise. The latter is also not an issue because the integration bandwidth is limited to a channel bandwidth B of only 200 kHz.

Equation (1.4) can be used to evaluate the required phase noise level \mathcal{L} at a given offset. Taking $B \cong 200$ kHz and a minimum signal-to-noise ratio $\text{SNR}|_{\text{dB}} = 9$ dB, the resulting LO phase-noise requirements have been organized in Table 1.2. Assuming a $1/\omega_m^2$ phase-noise

Table 1.2 Local oscillator phase-noise requirements for GSM at some frequencies

f_m (MHz)	Blocker power (dBm)	$\mathcal{L}(f_m)$ (dBc/Hz)
3	-23	-138
1.6	-33	-128
0.6	-43	-118